

χ PT Calculations with two-pion Loops for S-wave π^0 Production in pp Collision

E. Gedalin^{*}, A. Moalem[†] and L. Razdolskaya[‡]

Department of Physics, Ben Gurion University, 84105 Beer Sheva, Israel

Abstract

The total cross section for the $pp \rightarrow pp\pi^0$ reaction at energies close to threshold is calculated within the frame of a chiral perturbation theory, taking into account tree and one loop diagrams up to chiral order $D = 2$. Two-pion loop contributions dominate π^0 production at threshold. The calculated cross section reproduces data, both scale and energy dependence, fairly well.

Key Words : Chiral Perturbation, Two-pion loops, π^0 Production.

13.75.Cs, 14.40.Aq, 25.40.Ep

Typeset using REVTeX

^{*}gedal@bgumail.bgu.ac.il

[†]moalem@bgumail.bgu.ac.il

[‡]ljuba@bgumail.bgu.ac.il

In recent contributions [1–3], the cross section for the $pp \rightarrow pp\pi^0$ reaction at energies near threshold was calculated within the frame work of chiral perturbation theory (χ PT). Although χ PT accounts for all effects such as unitarity, spontaneously broken chiral symmetry and offshellness, the calculations in Refs. [1–3] underestimate the cross section data by a factor of 3-6. This stands in marked difference with the results from traditional one-boson exchange (OBE) model calculations, where contributions from heavy meson exchanges seem to resolve the discrepancy between predictions and data [4–6]. Particularly, in a fully covariant OBE model [6], the production amplitude is found to be dominated by a t-pole term, where the pion production occurs on an internal meson line at a $\pi\pi\sigma$ - meson vertex. Such a mechanism simulates contributions from two-pion exchanges and accounts effectively for two-pion loop diagrams. It is the purpose of the present note to show that the failure of χ PT calculations [1–3] to reproduce data may not be due to limitations of theory but to inconsistencies in the way χ PT was applied to this process and, that including two-pion loop contributions properly may resolve the discrepancy between predictions and data.

We carry out χ PT calculations up to chiral order $D = 2$, taking into account tree and one loop diagrams involving pions and nucleons only. The more important of these are depicted in Fig. 1. Many other loop diagrams (not shown in Fig. 1) contribute very little or/and renormalize the masses and coupling constants. The graphs 1a - 1c are the usual impulse and rescattering diagrams considered in Refs. [1–3]. The loop diagrams 1d - 1f correspond to two-pion exchanges in t-channels with isoscalar-scalar quantum numbers. Note that the contribution from graphs 1a-1f can be factorized into a pion source , a propagator and an off mass shell amplitude for the conversion process $\pi^0 p \rightarrow \pi^0 p$. We shall demonstrate below that this amplitude is strongly enhanced due to offshellness. The other graphs 1g and 1h are contributions specific to the production process, and can not be described in terms of one meson exchanges. The latter is a short-range interaction mechanism dictated by an order $D = 2$ χ PT Lagrangian.

A meson production in NN collisions necessarily involves large momentum transfer and two-pion loops like graphs 1d-1g are expected to play an important role. At threshold the

transferred momentum squared $q^2 = (p_3 - p_1)^2 \approx -Mm$, where M and m are masses of the nucleon and meson produced. It is to be demonstrated that the contribution from diagrams 1d-1f becomes very important off the mass shell, and thus providing the enhancement required to resolve the discrepancy between previous calculations and data.

We use the usual χ PT pion-nucleon sector heavy-fermion formalism (HFF) Lagrangian [7–9]

$$L = L^{(0)} + L^{(1)} + L^{(2)} , \quad (1)$$

where,

$$L^{(0)} = \frac{1}{2}[(\partial_\mu \pi)^2 - m^2 \pi^2] - \frac{1}{6F^2}[\pi^2(\partial_\mu \pi)^2 - (\pi \cdot \partial_\mu \pi)^2] + \frac{m^2}{4!F^2}(\pi^2)^2 + N^\dagger(iv\partial)N + N^\dagger \left\{ -\frac{1}{4F^2}\tau \cdot \pi \times (v\partial)\pi - \frac{1}{F}g_A S^\mu \tau \cdot [\partial_\mu \pi + \frac{1}{6F^2}(\pi\pi \cdot \partial_\mu \pi - \partial_\mu \pi \pi^2)] \right\} N; \quad (2)$$

$$L^{(1)} = \frac{1}{2M}(v^\mu v^\nu - g^{\mu\nu}) \left[N^\dagger \partial_\mu \partial_\nu N + \frac{1}{4F^2}(iN^\dagger \tau \cdot \pi \times \partial_\mu \pi \partial_\nu N + h.c.) \right] + \frac{g_A}{2MF}[iN^\dagger \tau(v\partial\pi)S^\mu \partial_\mu N + h.c.] + \frac{1}{2MF^2}N^\dagger[(c'_2 - \frac{1}{4}g_A^2)(v\partial\pi)^2 - c'_3(\partial_\mu \pi)^2 - 2c'_1 m^2 \pi^2]N + \dots , \quad (3)$$

and

$$L^{(2)} = -\frac{d_1}{2MF}[iN^\dagger \tau(v\partial\pi)S^\mu \partial_\mu N N^\dagger N + h.c.] + \dots \quad (4)$$

Here π and N represent pion and nucleon fields, v is the nucleon four velocity, $(v\partial) = v^\mu \partial_\mu$, F and g_A are the pion radiative decay and axial vector coupling constants. The dimensionless low energy coupling constants, $c'_1 = -1.63$, $c'_2 = 6.20$ and $c'_3 = -9.86$, are determined from fitting S-wave $\pi^0 N$ scattering data [9].

To consider the relative importance of the various graphs in Fig. 1, we apply the modified power counting scheme of Cohen et al. [2]. As already shown in Ref. [2], the impulse and rescattering terms (diagrams 1a-1c) are of the order $\sim (m/M)^{1/2}F^{-3}$ and $\sim (m/M)^{3/2}F^{-3}$, respectively. It is easy to show that the loop diagrams are of the same order of magnitude as the impulse term. Consider for example diagram 1d for which the characteristic momentum

squared is $Q^2 = (p_4 - p_2)^2 \approx -Mm$ (see Fig. 1 for notation). This graph depends upon πN as well as four pion interaction terms in $L^{(0)}$. From Eqn. 2, the πNN vertices contribute each a factor QF^{-1} while the four pion vertex contributes a factor Q^2F^{-2} . In addition there is a factor of Q^{-2} from each of the meson propagators, Q^{-1} from the internal nucleon line, and a factor of $Q^4(16\pi)^{-1}$ from the loop integral. Altogether, diagram 1d is of the order $\sim Q^2(16\pi F^5)^{-1} \sim mM(16\pi F^5)^{-1} \sim m(4F^4)^{-1}$. Numerically, $m/4F \approx (m/M)^{1/2}$ so that using the same organizing principle as in Ref. [2], diagram 1d is of the same order of magnitude as the impulse term, what brings us to conclude that loop diagrams should not be disregarded.

We now write the primary production amplitude for the $pp \rightarrow pp\pi^0$ reaction in the form

$$M^{(in)}(pp \rightarrow pp\pi^0) = M_I^{(1)} + M_R^{(1)} + M_L^{(1)} + M_L^{(2)} + M_S^{(2)}, \quad (5)$$

where

$$M_I^{(1)} = \frac{ig_A}{2F(q^2 - m^2)} \left\{ (-) \frac{g_A^2}{4MF^2} \mathbf{q}^2 \right\} \mathbf{p}\sigma_1 + [1 \leftrightarrow 2, 3 \leftrightarrow 4], \quad (6)$$

$$M_R^{(1)} = \frac{ig_A}{2F(q^2 - m^2)} \left\{ \frac{1}{MF^2} \left[(c'_2 + c'_3 - \frac{g_A^2}{4})mq^0 - 2c'_1m^2 \right] \right\} \mathbf{p}\sigma_1 + [1 \leftrightarrow 2, 3 \leftrightarrow 4], \quad (7)$$

$$M_L^{(1)} = \frac{ig_A}{2F(q^2 - m^2)} \left\{ \frac{g_A^2}{6F^4} (6mq^0 - 2q^2 - \frac{5}{2}m^2)B(Q^2) \right\} \mathbf{p}\sigma_1 + [1 \leftrightarrow 2, 3 \leftrightarrow 4], \quad (8)$$

$$M_L^{(2)} = -i \frac{1}{24F^5} g_A^3 B(Q^2) \mathbf{p}\sigma_1 + [1 \leftrightarrow 2, 3 \leftrightarrow 4], \quad (9)$$

$$M_S^{(2)} = i \frac{d_1 m}{2FM} \mathbf{p}\sigma_1 + [1 \leftrightarrow 2, 3 \leftrightarrow 4]. \quad (10)$$

Here the quantities $M_I^{(1)}$, $M_R^{(1)}$, $M_L^{(1)}$ denote the contributions from the impulse, rescattering and one-loop diagrams 1d-1f. These are written in a factorized form where the expressions in the curly brackets represent analogous contributions to the conversion process $\pi^0 p \rightarrow \pi^0 p$. $M_L^{(2)}$ and $M_S^{(2)}$ are the contributions from graphs 1g and 1h. Our notation is : $p = (M + \mathbf{p}^2/2M, \mathbf{p})$ and $k = (\sqrt{m^2 + \mathbf{k}^2/2M}, \mathbf{k})$ stand for the incoming proton and pion produced momenta in the overall center of mass (CM) frame; $Q = (-\mathbf{p}^2/2M, \mathbf{p})$ and $q = (-\mathbf{p}^2/2M, -\mathbf{p})$ are the transferred momenta. The bracket $[1 \leftrightarrow 2, 3 \leftrightarrow 4]$ represents the contribution from the same diagram with the proton momenta p_1 , p_3 interchanged with

p_2 , p_4 , respectively. The expressions for $M_I^{(1)}$, $M_R^{(1)}$ and $M_S^{(2)}$ are identical with those obtained by Cohen et al. [2]. The evaluation of the loop contribution, though a bit long and tedious, is straightforward and will not be given here. Both, $M_L^{(1)}$ and $M_L^{(2)}$ depend on the loop function defined to be [7,9]

$$B(q^2) = (-3 + 2\mathbf{p}^2 \frac{d}{dq^2}) B_0(q^2) , \quad (11)$$

$$B_0(q^2) = -\frac{1}{16\pi} \int_0^1 dz \sqrt{m^2 - q^2 z(1-z)} . \quad (12)$$

In the calculations to be presented below the values of constants and masses are taken to be : $F = 93 \text{ MeV}$, $m = 135 \text{ MeV}$, $M = 938 \text{ MeV}$ and $g_A = 1.26$. The short range interaction d_1 parameter is not determined by chiral symmetry. In order to fix its value we follow a procedure similar to that applied in Ref. [2], assuming that the short-range interactions originate from ρ and ω vector meson exchanges as depicted in Fig. 2. This leads to

$$d_1 = \frac{f_{\pi NN} F}{2mM} \left(\frac{g_{\rho NN}^2 (1 + \kappa)}{m_\rho^2 + Mm} + \frac{g_{\omega NN}^2}{m_\omega^2 + Mm} \right) . \quad (13)$$

Here $m_\rho = 770 \text{ MeV}$, $m_\omega = 782 \text{ MeV}$ are masses of the ρ and ω mesons; $f_{\pi NN}$ the πNN pseudovector coupling constant; $g_{\rho NN}$ and $g_{\omega NN}$ the ρNN and ωNN vector coupling constants; κ the ratio of tensor to vector ρNN coupling constants. With these taken from the OBEP set of Machleidt [10] one obtains $d_1 = 1.16 \text{ fm}^3$, a value nearly identical with the strength derived in Ref. [2].

The various contributions to the production amplitude are drawn in Fig. 3 vs η , the maximum pion momentum in the overall CM frame. We confirm the observation of Ref. [2] that the rescattering, though enhanced by off shell effects, has an opposite sign to that of the impulse term. These two terms interfere destructively, and thus reinforcing the importance of the other terms. In fact these two together with $M_L^{(2)}$ and $M_S^{(2)}$, the terms from graphs 1g and 1h, cancel to large extent. The one-loop term $M_L^{(1)}$ is significantly more important than any of the other contributions. This may well be understood by considering the off mass shell behavior of the amplitude for the $\pi^0 p \rightarrow \pi^0 p$ conversion process. Using the expression

in the curly brackets of Eqn. 8, the one loop contribution to the on mass shell conversion amplitude amounts to $T_L^{(1)} = 3m^3/64\pi F^4 = 0.1 \text{ fm}$, a value already derived by Bernard et al. [9]. Off mass shell at $q = (-m/2, -\sqrt{Mm})$ this term becomes rather large

$$T_L^{(1)} = g_A^2 MmB(-Mm(1 - m/4M))/3F^4 \approx 2.43 \text{ fm} . \quad (14)$$

Using Eqns. 6-7, the analogous quantities from the impulse and rescattering terms are $T_I^{(1)} = -1.21 \text{ fm}$ and $T_R^{(1)} = 0.54 \text{ fm}$, respectively. Thus off mass shell two-pion loop contributions dominate the conversion process also, with ratios $M_I^{(1)} : M_L^{(1)} : M_R^{(1)} \approx T_I^{(1)} : T_R^{(1)} : T_L^{(1)} \approx 5 : 2 : 1$.

In Fig. 4 we draw predictions for the total cross section of the $pp \rightarrow pp\pi^0$ reaction along with the data of Refs. [11,12]. Final state interactions (FSI) influence the energy dependence as well as the scale of the cross section. We treat FSI in an approximate way by assuming factorization of the S-wave production amplitude into a primary production amplitude, $M^{(in)}$ of Eqn. 5, and an S-wave FSI factor. For a three body process as in our case, the latter is identified [13] with the (on mass shell) amplitude for $\pi NN \rightarrow \pi NN$ elastic scattering. We have documented this approximation in length elsewhere [14,6] and shall skip further details here. We stress though that, applying this approximation to $pp \rightarrow pp\pi^0$ yield very similar corrections in comparison with those obtained with FSI between the two charged protons only [3,5,12]. The cross section calculated with the full amplitude of Eqn. 5 and with FSI corrections is drawn as a solid line in Fig. 4. Without contributions from loop diagrams the cross section (small dashed curve) is lower by a factor of ≈ 2.5 . To account for the initial and final pp interactions Sato et al. [3] have used distorted waves obtained by solving the Shrödinger equation with NN potential. These distorted waves are then used to calculate the matrix elements of the impulse and rescattering terms. It is very reassuring that the total cross section they have calculated (the solid line in their Fig. 4) is very close to our predictions (small dashed curve). The cross section calculated without FSI corrections (long dashed line with the full amplitude; dot-dashed curve without loop contributions) vary fast with energy due to phase space factor and does not account neither for the energy

dependence nor for the scale.

In summary we have calculated S-wave pion production in $pp \rightarrow pp\pi^0$ taking into account tree and one loop diagrams up to chiral order D=2. We have found that loop diagrams contribute significantly to the process. Dynamically, this means that two-pion exchanges play an essential role in the production process.

The calculations presented above can be improved by including contributions from other degrees of freedom. For example, excitations from the Δ (1232 MeV) nucleon isobar may well contribute to any of the graphs a-g in Fig. 1. In view of the large cancellations between the various contributions considered above it remains still to be verified that the HFF expansion converges. Finally, since contributions from D=2 loop diagrams have the same order of magnitude as those from lower order terms then it would be important to ascertain convergence of the next D=3 chiral order diagrams as well.

Acknowledgments This work was supported in part by the Israel Ministry Of Absorption. We are indebted to Z. Melamed for assistance in computation.

REFERENCES

- [1] B. -Y. Park et al., Phys. Rev. **C53**, 1519 (1996).
- [2] T. D. Cohen et al., Phys. Rev. **C53**, 2661 (1996).
- [3] T. Sato et al., Phys. Rev. **C56**, 1246 (1997).
- [4] T. S. H. Lee and D. Riska, Phys. Rev. Lett. **70**, 2237 (1993).
- [5] C. J. Horowitz et al., Phys. Rev. **C49**, 1337 (1994).
- [6] E. Gedalin, A. Moalem and L. Razdolskaya, nucl-th/9611005, and E. Gedalin, A. Moalem and L. Razdolskaya, submitted to Nucl. Phys. **A**.
- [7] T.S. Park, D. -P. Min and M.Rho, Phys. Rep. **233**, 341 (1993).
- [8] V. Bernard, N. Kaiser, T. -S. H. Lee, and Ulf-G. Meissner, Phys. Rep. **246**, 315 (1994).
- [9] V. Bernard, N. Kaiser and Ulf-G.Meissner, Int. J. Mod. Phys. **E4**, 193 (1995).
- [10] R. Machleidt , Adv. in Nucl. Phys.**19**(1989) 189 .
- [11] A. Bondar et al., Phys. Lett. **B356**, 8 (1995).
- [12] H. O. Meyer et al., Nucl. Phys. **A539**, 683 (1992).
- [13] A. Moalem, L. Razdolskaya and E. Gedalin, hep-ph/9505264;
A. Moalem, E. Gedalin, L. Razdolskaya and Z. Shorer, π N Newsletter Proceeding of
the 6th International Symposium on Meson-Nucleon Physics and the Structure of the
Nucleon, **10**, 172 (1995).
- [14] A. Moalem, E. Gedalin, L. Razdolskaya and Z. Shorer, Nucl. Phys. **A589**, 649 (1995);
A. Moalem, E. Gedalin, L. Razdolskaya and Z. Shorer, Nucl. Phys. **A600**, 445 (1996).

FIGURES

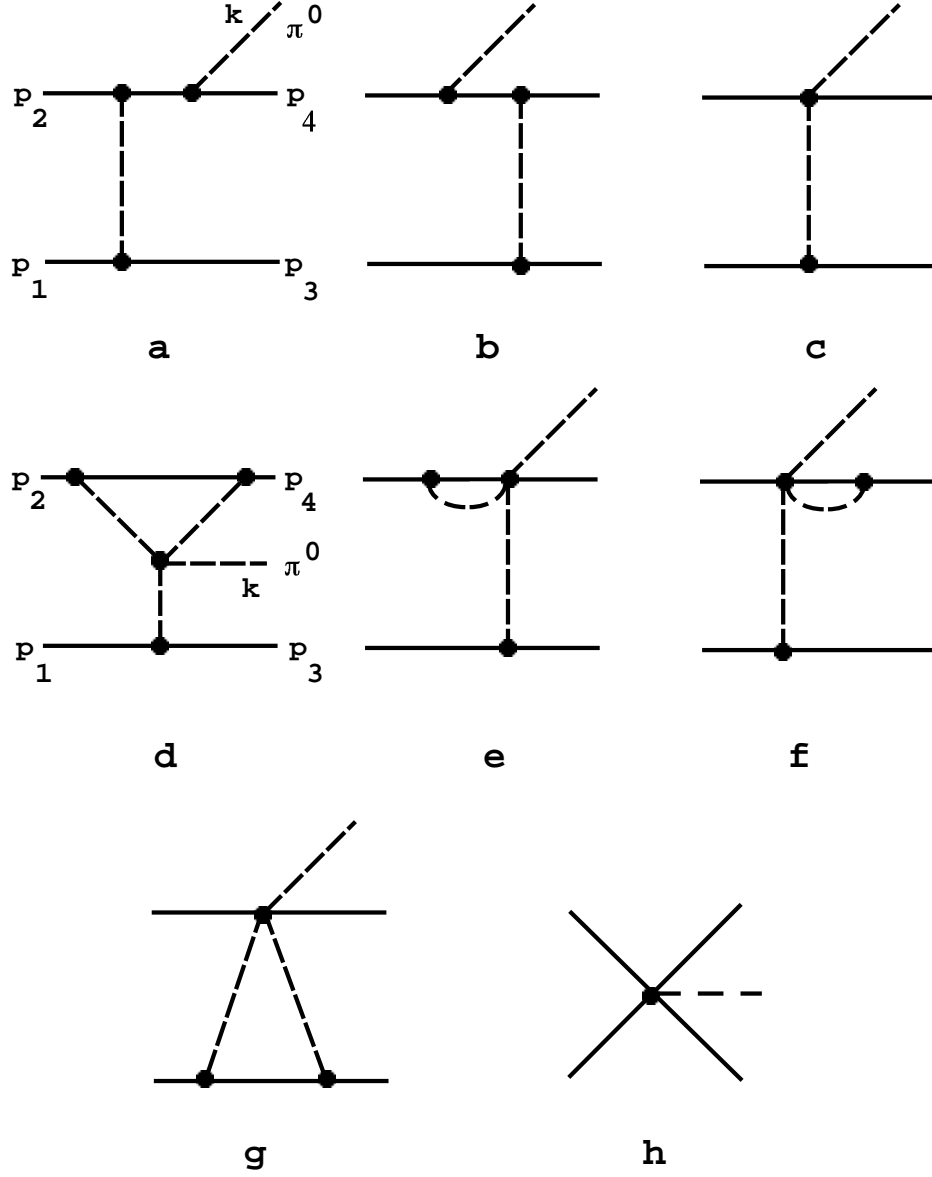


FIG. 1. Various contributions to the $NN \rightarrow NN\pi^0$ reaction. In this and following figure a solid line stands for a nucleon and a dashed line represents a meson.

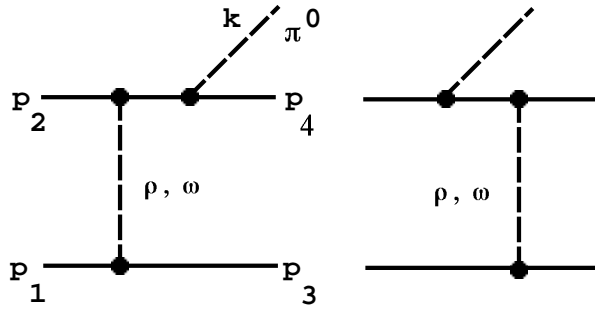


FIG. 2. The meson-exchange mechanism used to model the short-range interaction. Contributions from both ρ and ω mesons are considered.

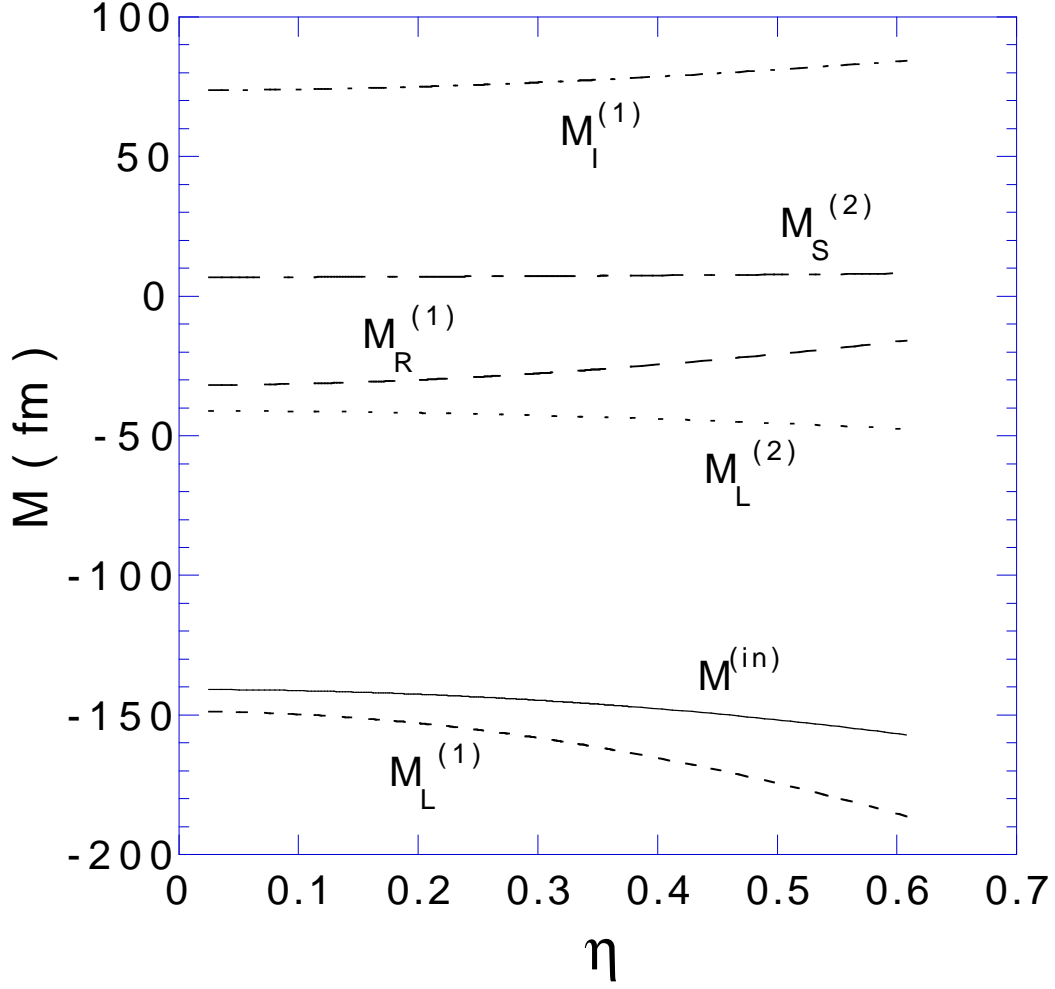


FIG. 3. Various partial amplitudes for the $pp \rightarrow pp\pi^0$ reaction vs. η the maximum pion momentum in the overall CM frame. The curves labeled, $M_I^{(1)}$, $M_R^{(1)}$, $M_S^{(2)}$, $M_L^{(1)}$ and $M_L^{(2)}$ are due to the impulse, rescattering, short range interaction and loop contributions. (see text for details).

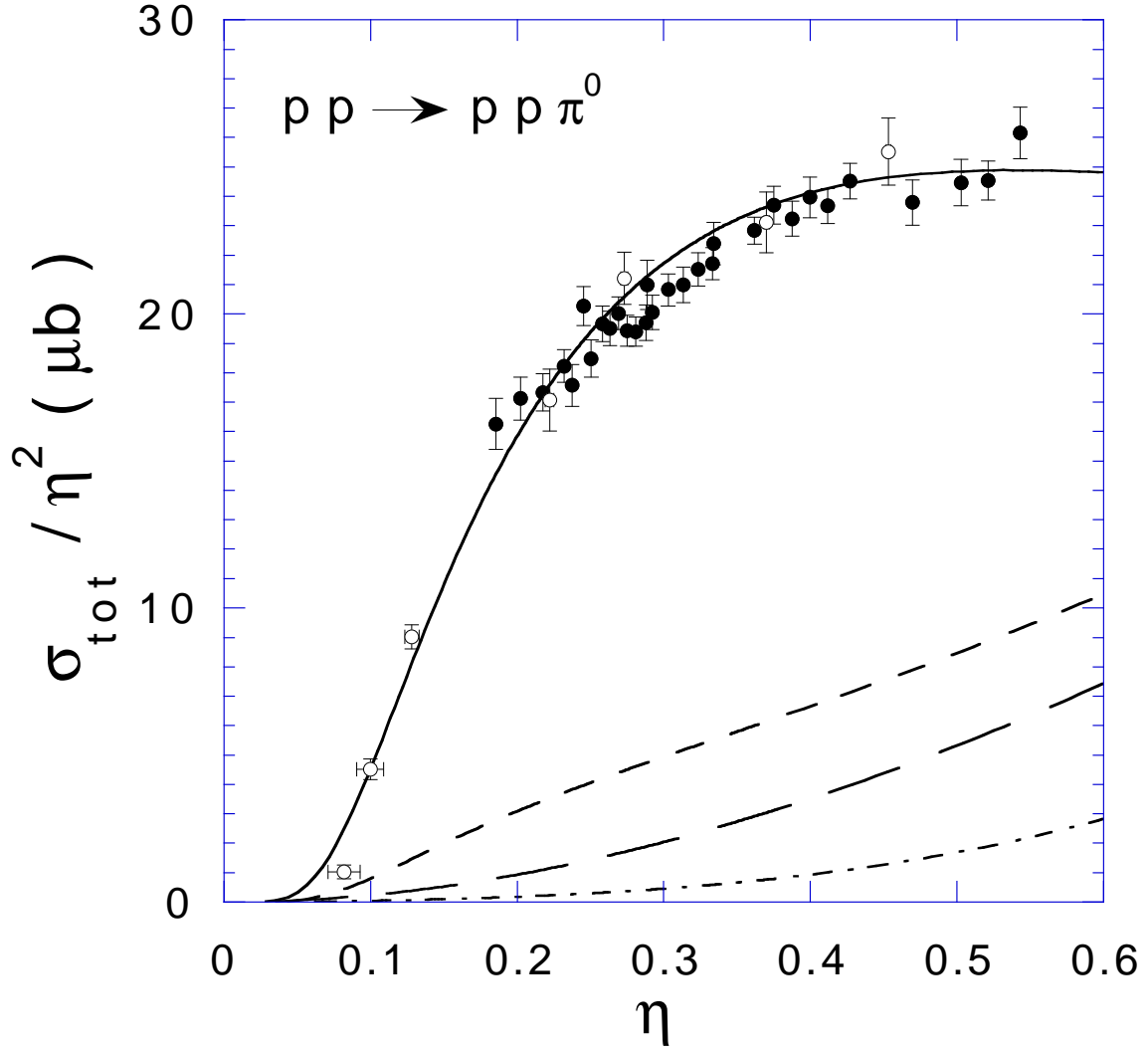


FIG. 4. Predictions for the total cross section vs. η , the maximal pion momentum in the overall CM frame. Predictions corrected for FSI with (full amplitude of Eqn. 5) and without loop contributions are drawn as solid line and small dashed curves, respectively. Predictions without FSI corrections are drawn as long dashed (full amplitude) and dot-dashed (loop contributions not included).